Biophysical Journal, Volume *116*

Supplemental Information

A Biomechanical Model of Tumor-Induced Intracranial Pressure and Edema in Brain Tissue

Inmaculada C. Sorribes, Matthew N.J. Moore, Helen M. Byrne, and Harsh V. Jain

SUPPLEMENTAL INFORMATION

S1 Numerical Test Problem

Consider the heat equation on the shrinking domain $0 \le x \le G(t)$:

$$\begin{aligned} [h]_t &= [h]_{xx}, && t > 0, 0 < x < G(t), \\ [h]_x &= 0, && t > 0, x = 0, \\ [h]_x + \dot{G(t)}h &= 0, && t > 0, x = G(t), \\ h(x,0) &= h_\infty, && 0 < x < G(t). \end{aligned} \tag{S1.1}$$

Using Reynold's transport theorem, as well as the boundary conditions we can show conservation of mass:

$$\begin{aligned} \frac{d}{dt}\int_0^{G(t)} h(x,t)dx &= \int_0^{G(t)} [h]_t dx + \dot{G(t)}h(x = G(t), t), \\ &= \int_0^{G(t)} [h]_{xx} dx + \dot{G(t)}h(x = G(t), t), \\ &= [h]_x(x = G(t), t) - h_x(x = 0, t) + \dot{G(t)}h(x = G(t), t), \\ &= [h]_x(x = G(t), t) + \dot{G(t)}h(x = G(t), t), \\ &= 0. \end{aligned}$$

Applying the change of variables presented in the manuscript (15) to (S1.1) leads to:

$$\begin{aligned} [h]_t &= [u]_y[y]_t + [u]_s[s]_t, \\ &= [u]_y\Big(\frac{-xG\dot{(s)}}{(G(s))^2}\Big) + [u]_s, \\ &= [u]_y\Big(\frac{-yG\dot{(s)}}{G(s)}\Big) + [u]_s. \\ [h]_x &= [u]_y[y]_x + [u]_s[s]_x, \\ &= [u]_y\Big(\frac{1}{G(s)}\Big). \\ [h]_{xx} &= [u]_{yy}\Big(\frac{1}{(G(s))^2}\Big). \end{aligned}$$

Thus, the system in the transformed domain reduces to:

$$\begin{aligned} [u]_s - \Big(\frac{yG\dot{(s)}}{G(s)}\Big)[u]_y &= \Big(\frac{1}{(G(s))^2}\Big)[u]_{yy}, && s > 0, 0 < y < 1, \\ [u]_y &= 0, && s > 0, y = 0, \\ [u]_y &= -\dot{G(s)}G(s)u, && s > 0, y = 1, \\ u(y,0) &= u_\infty, && 0 < y < 1. \end{aligned} \tag{S1.2}$$

Since we know mass is preserved in the decreasing boundary, we can calculate how the mass in the fixed domain is varying:

$$\frac{d}{dt}\int_0^1 u(y,s)dy = \int_0^1 [u]_s dy, \tag{S1.3}$$

$$= \int_0^1 \Big(\Big(\frac{yG\dot{(s)}}{G(s)}\Big)[u]_y + \Big(\frac{1}{(G(s))^2}\Big)[u]_{yy}\Big)dy,$$

$$= \frac{\dot{G(s)}}{G(s)}yu\Big|_0^1 - \frac{\dot{G(s)}}{G(s)}\int_0^1 udy + \frac{1}{(G(s))^2}(-G(s)\dot{G(s)}u(y = 1, s)),$$

$$= -\frac{\dot{G(s)}}{G(s)}\int_0^1 udy.$$

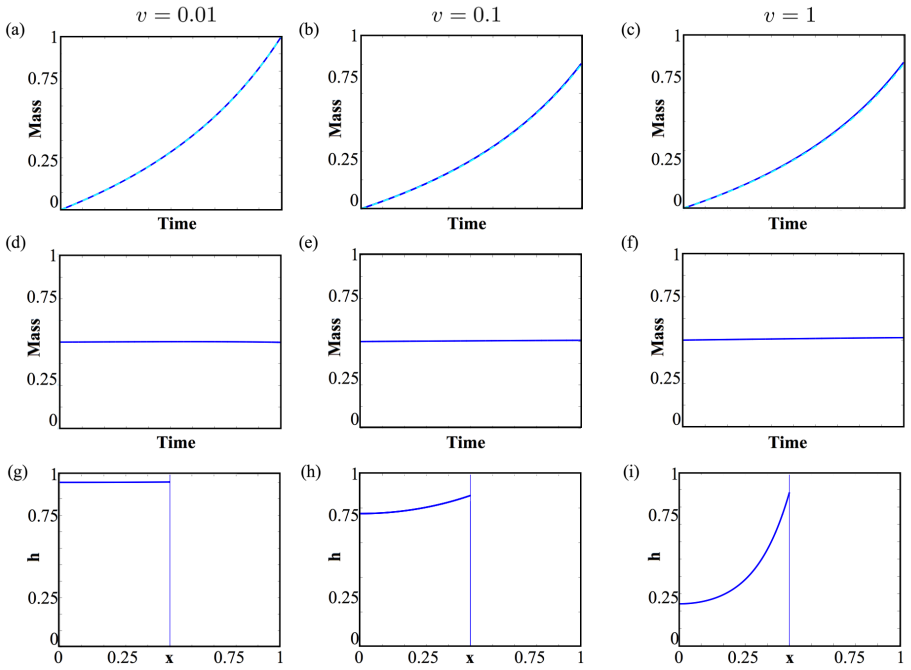

Figure S1.1: (a)-(c) Plots of total mass versus time. Total mass of $u(s, y)$ was calculated by integrating over space. Simulations of (S1.5) is shown in a solid blue curve, and the theoretical mass increase in a dashed cyan curve taking (a) $v = 0.01$, (b) $v = 0.1$, and (c) $v = 1$. (d)-(f) Plots of total mass versus time. Total mass of $h(x, t)$ was calculated by integrating over space the solution of (S1.1) when (d) $v = 0.01$, (e) $v = 0.1$, and (f) $v = 1$. (g)-(i) Plots of $h(x, t)$ versus x. In each case, different rates v of tumor growth are considered ((g): $v = 0.01$, (h): $v = 0.1$, and (i): $v = 1$). Simulations of (S1.1) were run until the tumor boundary reaches $x = 0.5$. The vertical lines denote the position of the tumor.

If we now solve:

$$\begin{aligned} \frac{d}{dt}\int_0^1 u(y,s)dy &= -\frac{\dot{G(s)}}{G(s)}\int_0^1 u dy, \\ \ln\left(\int_0^1 u(y,s)dy\right) &= -\ln(G(s)) + K, \\ \int_0^1 u(y,s)dy &= \frac{u_\infty}{G(s)}. \end{aligned} \tag{S1.4}$$

Considering $G(t) = 1 - vt$, since this is the function we use in our original problem, the system reads:

$$\begin{aligned} [u]_s + \left(\frac{yv}{1-vs}\right)[u]_y &= \left(\frac{1}{(1-vs)^2}\right)[u]_{yy}, && s > 0, 0 < y < 1, \\ [u]_y &= 0, && s > 0, y = 0, \\ [u]_y &= v(1-vs)u, && s > 0, y = 1, \\ u(y,0) &= u_\infty, && 0 < y < 1. \end{aligned} \tag{S1.5}$$

We tested that our numerical scheme shows conservation of mass for three different velocities $v = 0.01, 0.1, 1$ (figure S1.1(d), (e), and (f)). Figure S1.1(a), (b), and (c) show that the increase in mass of the numerical simulation corresponds to the calculated increase in (S1.4). In both figures the numerical simulation is presented in a solid blue curve and the theoretical result in a dashed cyan curve.

S1.1 Test Problem Asymptotic Approximation

Based on numerical simulations of (S1.1), we observe that when v is small $h(x, t)$ grows evenly throughout the domain. In order to study this behavior, we consider $v = O(\epsilon)$, and we rescale time to the same order as v, that is $\tau = \epsilon t$. Under these assumptions S1.1 reads:

$$\begin{aligned} \epsilon[h]_\tau &= [h]_{xx}, && \tau > 0, 0 < x < 1 - \tau, \\ [h]_x &= 0, && \tau > 0, x = 0, \\ [h]_x &= vh, && \tau > 0, x = 1 - \tau, \\ h(x,0) &= h_\infty, && 0 < x < 1 - \tau. \end{aligned}$$

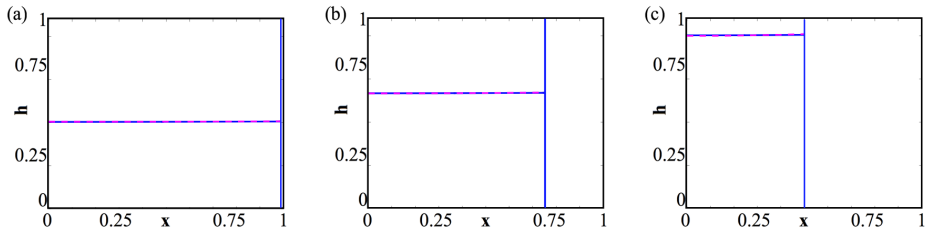

Figure S1.2: Plots of $h(x,t)$ versus x by simulating (S1.1) is presented in a blue solid curve along with the asymptotic approximation (S1.6) in a dashed magenta curve. We captured both at an early (a), intermediate (b), and late time (c).

By seeking solutions of the form $h = h_0(x,\tau) + vh_1(x,\tau) + v^2h_2(x,\tau) + v^3h_3(x,\tau) + O(^4)$ at leading order:

$$h_0(\tau) = \frac{h_\infty}{1-\tau}.$$

The first correction term $h_1(x,\tau)$ can be calculated:

$$[h_1]_{xx} = [h_0]_\tau = \frac{vh_\infty}{(1-\tau)^2},$$
$$h_1(x,\tau) = \frac{x^2h_\infty}{2(1-\tau)^2}.$$

As well as:

$$[h_2]_{xx} = [h_1]_\tau = \frac{v^2x^2h_\infty}{(1-\tau)^3},$$
$$h_2(x,\tau) = \frac{x^4h_\infty}{12(1-\tau)^3}.$$

Similarly we can continue calculating correction terms. The asymptotic solution with three correction terms reads:

$$h(x,\tau) \sim \frac{h_\infty}{1-vt} + v\frac{x^2h_\infty}{2(1-vt)^2} + v^2\frac{x^4h_\infty}{12(1-vt)^3} + v^3\frac{x^6h_\infty}{120(1-vt)^4}. \tag{S1.6}$$

Figure S1.2 shows the numerical solution (blue solid curve) along with the asymptotic approximation (dashed magenta curve). We captured both at an early (figure S1.2(a)), intermediate (figure S1.2(b)), and late time (figure S1.2(c)).

S2 Conservation of Mass

If ρ is taken to be zero in equations (14) we can show conservation of mass in the system. First, we consider the additional isotropic pressure to be constant, $\Gamma(h) = \gamma$. Non-dimentionalizing (14) by taking $t = \frac{L^2}{\gamma}t^*$, $v = \frac{\gamma}{L}v^*$, and $x = Lx^*$ we obtain:

$$\begin{aligned}
[h]_{t^*} &= (1-h)[h]_{x^*x^*} - ([h]_{x^*})^2 + \rho^*(1-h)h, && t^* > 0, 0 < x^* < 1,\\
[h]_{x^*} &= 0, && t^* > 0, x^* = 0,\\
[h]_{x^*} &= v^*\frac{h}{(1-h)}, && t^* > 0, x^* = 1 - v^*t^*,\\
h(x^*,0) &= h_\infty, && 0 < x^* < 1.
\end{aligned} \tag{S2.7}$$

For now on, we drop the asterisks for convenience. Using the change of variables (15) the system in the fixed domain reads:

$$\begin{aligned}
[u]_s + \Big(\frac{yv}{1-vs}\Big)[u]_y &= (1-u)\frac{1}{(1-vs)^2}[u]_{yy} - \frac{1}{(1-vs)^2}([u]_y)^2 + \rho(1-u)u, && s > 0, 0 < y < 1,\\
[u]_y &= 0, && s > 0, y = 0,\\
[u]_y &= (1-vs)v\frac{u}{1-u}, && s > 0, y = 1,\\
u(y,0) &= u_\infty, && 0 < y < 1.
\end{aligned} \tag{S2.8}$$

Using Reynold's theorem:

$$\begin{aligned}
\frac{d}{dt}\int_0^{1-vt} h(x,t)dx &= \int_0^{1-vt} [h]_t dx - vh(x=1-vt,t),\\
&= \int_0^{1-vt} \Big([h]_{xx} - h[h]_{xx} - ([h]_x)^2\Big)dx - vh(x=1-vt,t),\\
&= \int_0^{1-vt} \Big([h]_{xx} - [h[h]_x]_x\Big)dx - vh(x=1-vt,t),\\
&= (1-h(x=1-vt,t))[h]_x(x=1-vt,t) - vh(x=1-vt,t),\\
&= 0.
\end{aligned}$$

Which shows conservation of mass. Now consider (S2.8). As we did before:

$$\begin{aligned}
\frac{d}{ds}\int_0^1 u(y,s)dy &= \int_0^1 [u]_s dy,\\
&= \int_0^1 \Big(\Big(-\frac{yv}{1-vs}\Big)[u]_y + (1-u)\frac{1}{(1-vs)^2}[u]_{yy} - \frac{1}{(1-vs)^2}([u]_y)^2\Big)dy,\\
&= \int_0^1 \Big(\Big(-\frac{yv}{1-vs}\Big)[u]_y + \frac{1}{(1-vs)^2}[u]_{yy} - \frac{1}{(1-vs)^2}[u[u]_y]_y\Big)dy,\\
&= -\frac{v}{1-vs}u(y=1,s) - \frac{v}{1-vs}\int_0^1 u dy + \frac{1}{(1-vs)^2}[u]_y(y=1,s)\\
&- \frac{1}{(1-vs)^2}u(y=1,s)[u]_y(y=1,s),\\
&= -\frac{v}{1-vs}\int_0^1 u(y,s)dy.
\end{aligned}$$

If we now solve:

$$\begin{aligned}
\frac{d}{ds}\int_0^1 u(y,s)dy &= -\frac{v}{1-vs}\int_0^1 u(y,s)dy,\\
\ln\Big(\int_0^1 u(y,s)dy\Big) &= -\ln(1-vs) + K,\\
\int_0^1 u(y,s)dy &= \frac{u_\infty}{1-vs}.
\end{aligned}$$

In figure S2.3(b), (d), and (f) we show that our numerical solution has conservation of mass. For illustrative purposes we picked $v = 0.01, 0.1, 1$ respectively. Figure S2.3(a), (b), and (e) present the numerical solution in a solid blue line, as well as the theoretical result in a dashed cyan line. We can see that, as v increases, the numerical solution becomes less accurate. This problem can be overcome, to an extent, by refining the mesh size.

Following a similar process, we can show conservation of mass when $\Gamma(h) = \gamma h/(1-h)$ (figure S2.4(b), (d), and (f)). Figure S2.4(a), (b), and (e) present the numerical solution in a solid blue line, as well as the theoretical result in a dashed cyan line. The velocity was taken to be $v = 0.01, 0.1, 1$ respectively.

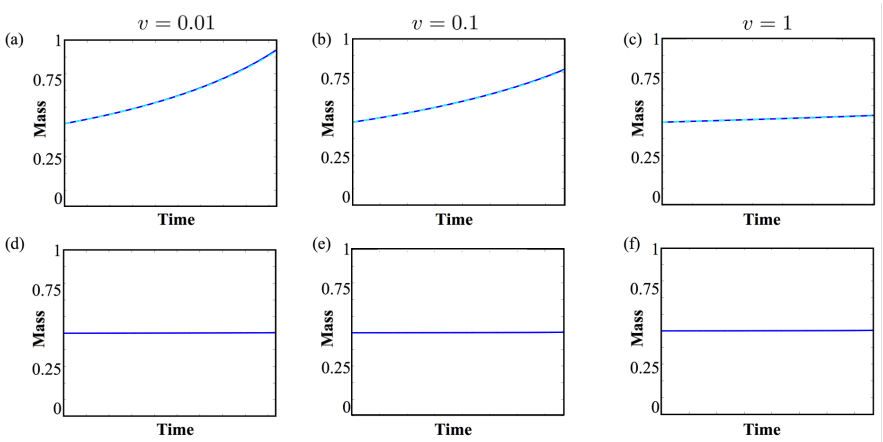

Figure S2.3: (a)-(c) Plots of total mass versus time. Total mass of $u(s, y)$ was calculated by integrating over space. Simulations of (S2.8) is shown in a solid blue curve, and the theoretical mass increase in a dashed cyan curve taking (a) $v = 0.01$, (b) $v = 0.1$, and (c) $v = 1$. (d)-(f) Plots of total mass versus time when $\rho = 0$. Total mass of $h(x, t)$ was calculated by integrating over space when (d) $v = 0.01$, (e) $v = 0.1$, and (f) $v = 1$.

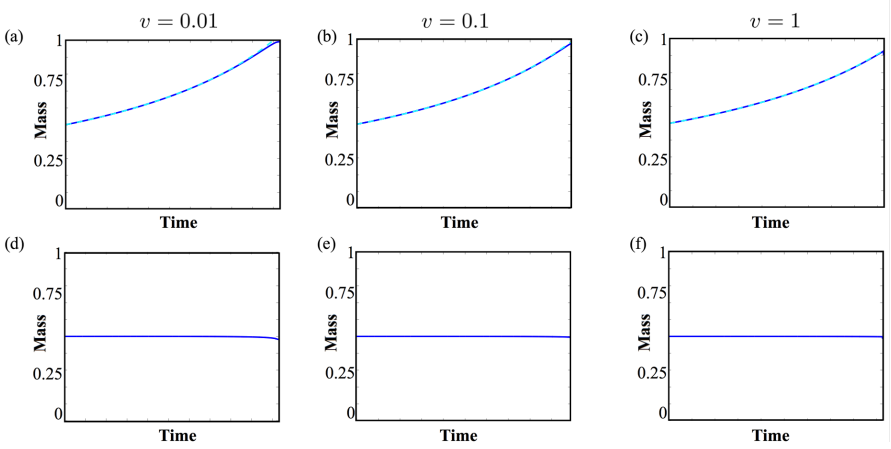

Figure S2.4: (a)-(c) Plots of total mass versus time. Total mass of $u(s, y)$ was calculated by integrating over space. Simulations of (S2.8) is shown in a solid blue curve, and the theoretical mass increase in a dashed cyan curve taking (a) $v = 0.01$, (b) $v = 0.1$, and (c) $v = 1$. (d)-(f) Plots of total mass versus time when $\rho = 0$. Total mass of $h(x, t)$ was calculated by integrating over space the solution of (14) when (d) $v = 0.01$, (e) $v = 0.1$, and (f) $v = 1$.

Once we introduce remodeling we cannot obtain a functional form of the change in mass:

$$\begin{aligned}
\frac{d}{dt}\int_0^{1-vt} h(x,t)dx &= \int_0^{1-vt} [h]_t dx - vh(x=1-vt,t),\\
&= \int_0^{1-vt} \Big([h]_{xx} - h[h]_{xx} - ([h]_x)^2 + \rho\Big(1-\frac{h}{h_\infty}\Big)h\Big)dx - vh(x=1-vt,t),\\
&= \int_0^{1-vt} \Big([h]_{xx} - [h[h]_x]_x + \rho\Big(1-\frac{h}{h_\infty}\Big)h\Big)dx - vh(x=1-vt,t),\\
&= (1-h(x=1-vt,t))[h]_x(x=1-vt,t) - vh(x=1-vt,t)\\
&+ \int_0^{1-vt} \rho\Big(1-\frac{h}{h_\infty}\Big)h dx\\
&= \int_0^{1-vt} \rho\Big(1-\frac{h}{h_\infty}\Big)h dx.
\end{aligned}$$

S3 Alternative Model Simplification

Here we present the alternative derivation of the model, where we solve for w instead of h. As we did previously, we eliminate $h = 1 - w$ from the model equations via the "no voids" assumption in (3). Then, adding (1) and (2):

$$[v_h h + v_w w]_x = 0 \tag{S3.9}$$

Integrating the above with respect to x and recalling that the skull (at $x = 0$) is impermeable to fluid and tissue, we obtain:

$$v_h = \frac{-w}{1-w} v_w. \tag{S3.10}$$

Following the process we did in the main text, adding (5) and (6), and using (3) and (7)-(8), the momentum balance for the system in terms of w reduces to:

$$[p]_x = -[(1-w)\Gamma(1-w)]_x, \tag{S3.11}$$

that is $p(x,t) = -(1-w)\Gamma(1-w) + p_0(t)$. We now substitute from (4),(7),(9), (S3.10), and (S3.11) into (5) to obtain the following expression for the velocity of the tissue phase:

$$v_w = \frac{1}{k_{hw}}[(1-w)\Gamma(1-w)]_x. \tag{S3.12}$$

Again, the positive constant k_{hw} may be absorbed into $\Gamma(1-w)$ and therefore we neglect it in what follows. Finally, we substitute from (S3.10) into (2), to arrive at the following PDE:

$$\begin{aligned}
[w]_t &= -\Big[w[(1-w)\Gamma(1-w)]_x\Big]_x - \rho\Big(\frac{w-h_\infty}{1-h_\infty}\Big)(1-w), && 0<t<L/v, 0<x<L-vt,\\
w[(1-w)\Gamma(1-w)]_x &= 0, && 0<t<L/v, x=0,\\
w[(1-w)\Gamma(1-w)]_x &= -vw, && 0<t<L/v, x=L-vt,\\
w(x,0) &= 1-h_\infty, && 0\le x\le L.
\end{aligned} \tag{S3.13}$$

We remark that the boundary condition for the water phase w has the opposite sign to the boundary condition for the tissue phase h. This represents the flow of fluid towards the tumor region.

S4 Asymptotic Analysis

Here we elaborate on some of the asymptotic analysis done in section 3.

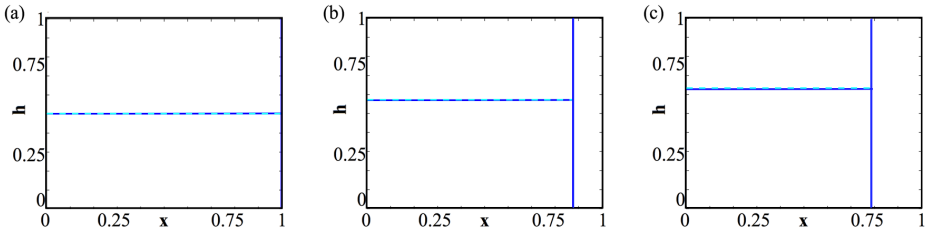

Figure S4.5: Asymptotic Approximation of Pilocytic Astrocytoma. Plots of $h(x,t)$ versus x by simulating (14) $\nu = O(\epsilon)$, $\rho = O(\epsilon^2)$, and $\gamma = O(1/\epsilon)$ is presented in a blue solid curve along with the asymptotic approximation (18) in a dashed cyan curve. Specifically, $\nu = 0.1, \rho = 0.01, \gamma = 10$. We captured both at an early (a), intermediate (b), and late time (c).

S4.1 Pilocytic Astrocytoma (grade I)

At leading order we obtain that:

$$\begin{aligned}\hat{\gamma}\Big[\frac{(2-h_0)h_0}{1-h_0}\frac{\partial h_0}{\partial x}\Big]_x &= 0, \quad t>0, 0<x<1-\hat{\nu}\tau\\ [h_0]_x &= 0, \quad x=0,\\ [h_0]_x &= 0, \quad x=1-\hat{\nu}\tau.\end{aligned}$$

Thus $h_0 = h_0(\tau)$ is independent of x. To obtain the functional form of h_0 we now study $O(\epsilon)$:

$$\begin{aligned}\hat{\gamma}\Big[\frac{(2-h_0)h_0}{1-h_0}\frac{\partial h_1}{\partial x}\Big]_x &= 0, \quad t>0, 0<x<1-\hat{\nu}\tau\\ [h_1]_x &= 0, \quad x=0,\\ [h_1]_x &= 0, \quad x=1-\hat{\nu}\tau.\end{aligned}$$

Therefore, not only the leading order is independent of space, but also the first correction term $h_1 = h_1(\tau)$. Considering higher order correction terms:

$$\begin{aligned}[h_0]_\tau &= \hat{\gamma}\Big[\frac{(2-h_0)h_0}{1-h_0}[h_2]_x\Big]_x, \quad t>0, 0<x<1-\hat{\nu}\tau\\ [h_2]_x &= 0, \qquad\qquad\qquad\qquad x=0,\\ [h_2]_x &= \frac{\hat{\nu}}{\hat{\gamma}}\frac{1-h_0}{2-h_0}, \qquad\qquad\qquad x=1-\hat{\nu}\tau.\end{aligned}$$

Thus:

$$h_2(x,\tau) = A(\tau)x + B(\tau) + f(h_0)\frac{x^2}{2}.$$

Where $A(\tau) = 0$ and:

$$f(h_0) = \frac{\hat{\nu}}{\hat{\gamma}}\frac{1-h_0}{2-h_0}\frac{1}{1-\hat{\nu}\tau}.$$

Which results in the close form of:

$$\begin{aligned}[h_0]_\tau &= \hat{\nu}\frac{h_0}{1-\hat{\nu}\tau},\\ \int\frac{dh_0}{h_0} &= \int\frac{\hat{\nu}}{1-\hat{\nu}\tau}d\tau,\\ h_0(\tau) &= \frac{C}{1-\hat{\nu}\tau}.\end{aligned}$$

Which using the initial condition leads to (18). In figure S4.5 numerical simulations using the numerical methodology proposed in section 2.3 are presented in a blue solid curve along with the asymptotic approximation (18) in a dashed cyan curve.

S4.2 Diffusive Astrocytoma (grade II)

In figure S4.6 numerical simulations using the numerical methodology proposed in section 2.3 are presented in a blue solid curve along with the asymptotic approximation (21) in a dashed cyan curve.

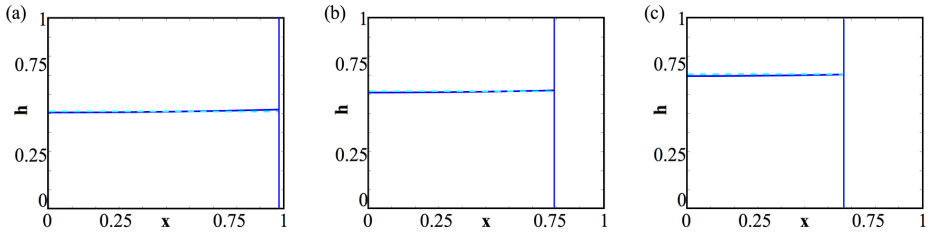

Figure S4.6: Asymptotic Approximation of Diffusive Astrocytoma. Plots of $h(x,t)$ versus x by simulating (14) with $\nu = O(1)$, $\rho = O(1)$, and $\gamma = O(1/\epsilon)$ is presented in a blue solid curve along with the asymptotic approximation (21) in a dashed cyan curve. Specifically, $\nu = 1, \rho = 1, \gamma = 10$. We captured both at an early (a), intermediate (b), and late time (c).

S4.3 Anaplastic Astrocytoma (grade III)

The equations for the leading order will then read:

$$\begin{aligned} \hat{\gamma}\Big[\frac{(2-h_0)h_0}{1-h_0}[h_0]_x\Big]_x &= 0, && t>0, 0<x<1,\\ [h_0]_x &= 0, && t>0, x=0,\\ [h_0]_x &= 0, && t>0, x=1-\nu t. \end{aligned}$$

Thus, $h_0 = h_0(t)$ is independent of x. Now consider $O(\epsilon)$:

$$[h_0]_t = \hat{\gamma}\Big[\frac{(2-h_0)h_0}{1-h_0}[h_1]_x\Big]_x, \qquad t>0, 0<x<1, \tag{S4.14}$$

$$[h_1]_x = 0, \qquad t>0, x=0, \tag{S4.15}$$

$$[h_1]_x = \frac{\nu(1-h_0)}{\hat{\gamma}(2-h_0)}, \qquad t>0, x=1-\nu t. \tag{S4.16}$$

Since $h_0(t)$ is independent of space we can conclude that:

$$h_1(x,t) = A(t)x + B(t) + f(h_0)\frac{x^2}{2}. \tag{S4.17}$$

From (S4.15) we know that $A(t) = 0$ and from (S4.16):

$$\begin{aligned} \nu h_0 &= \hat{\gamma}\frac{(2-h_0)h_0}{1-h_0}(f(h_0)(1-\nu t)),\\ f(h_0) &= \frac{\nu}{\hat{\gamma}}\frac{1-h_0}{2-h_0}\frac{1}{1-\nu t}. \end{aligned}$$

Resulting in:

$$\begin{aligned} [h_0]_t &= \nu\frac{h_0}{1-\nu t},\\ \int\frac{dh_0}{h_0} &= \int\frac{\nu}{1-\nu t}dt,\\ h_0 &= \frac{C}{1-\nu t}. \end{aligned}$$

Which using the initial condition leads to (23). We can calculate the first correction term:

$$\begin{aligned} [h_1]_t &= \hat{\gamma}\Big[\frac{(2-h_0)h_0}{1-h_0}[h_2]_x + 2h_1[h_1]_x\Big]_x, && t>0, 0<x<1,\\ [h_2]_x &= 0, && t>0, x=0,\\ \hat{\gamma}\Big(\frac{(2-h_0)h_0}{1-h_0}[h_2]_x + 2h_1[h_1]_x\Big) &= \nu h_1, && t>0, x=1-\nu t. \end{aligned}$$

From before we had that:

$$h_1(x,t) = B(t) + f(h_0)\frac{x^2}{2}.$$

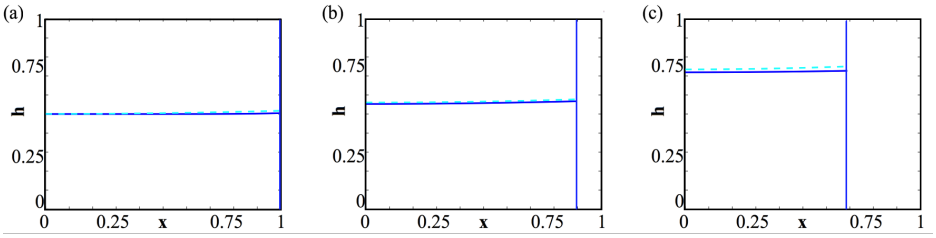

Figure S4.7: Asymptotic Approximation of Anaplastic Astrocytoma. Plots of $h(x,t)$ versus x by simulating (14) with $v = O(1)$, $\rho = O(\epsilon^2)$, and $\gamma = O(1/\epsilon)$ is presented in a blue solid curve along with the asymptotic approximation (24)-(23) in a dashed cyan curve. Specifically, $v = 1, \rho = 0.01, \gamma = 10$. We captured both at an early (a), intermediate (b), and late time (c).

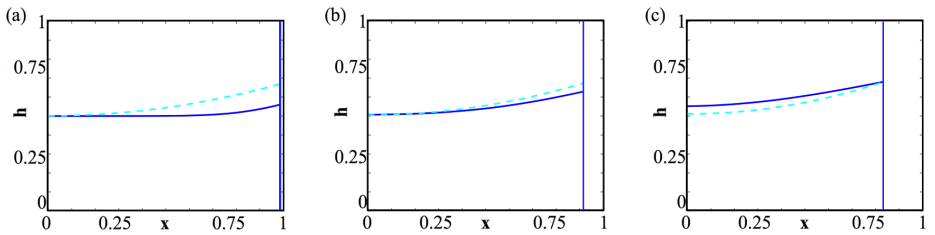

Figure S4.8: Asymptotic Approximation of Glioblastoma. Plots of $h(x,t)$ versus x by simulating (14) with $v = O(1/\epsilon)$, $\rho = 0$, and $\gamma = O(1/\epsilon)$ is presented in a blue solid curve along with the asymptotic approximation (26) in a dashed cyan curve. Specifically, $v = 10, \rho = 0, \gamma = 10$. We captured both at an early (a), intermediate (b), and late time (c).

where

$$f(h_0) = \frac{v}{\hat{\gamma}} \frac{1-h_0}{2-h_0} \frac{1}{1-vt},$$
$$f'(h_0) = \frac{v}{\hat{\gamma} h_\infty} \frac{h_0^2 - 4h_0 + 2}{(2-h_0)^2},$$

and

$$(h_1)^2 = (B(t))^2 + B(t) f(h_0) x^2 + (f(h_0))^2 \left(\frac{x^4}{4}\right),$$
$$[(h_1)^2]_x = 2B(t) f(h_0) x + (f(h_0))^2 x^3,$$
$$[(h_1)^2]_{xx} = 2B(t) f(h_0) + 3(f(h_0))^2 x^2.$$

Where $B(t)$ can be found:

$$B(t) = \frac{v}{48\hat{\gamma}} \left(\frac{1}{1-vt} \left(\frac{(h_\infty)^3}{(2(1-vt) - h_\infty)} + 4 - 2h_\infty - \frac{(h_\infty)^3}{2-h_\infty} \right) + 2h_\infty - 4(1-vt) \right).$$

Which gives us a functional form for the correction term $h_1(x,t)$. In figure S4.7 numerical simulations using the numerical methodology proposed in section 2.3 are presented in a blue solid curve along with the asymptotic approximation (23)-(24) in a dashed cyan curve.

S4.4 Glioblastoma Multiforme (grade IV)

In figure S4.8 numerical simulations using the numerical methodology proposed in section 2.3 are presented in a blue solid curve along with the asymptotic approximation (26) in a dashed cyan curve.

	Grade	γ	v	ρ
Pilocytic Astrocytoma	I	10	0.1	0.01
Diffusive Astrocytoma	II	10	1	1
Anaplastic Astrocytoma	III	10	1	0.01
Glioblastoma	IV	10	10	0

Table S4.1: Parameter Values for simulations in section 3 and S4.